Supernumerary Rainbows in the Angular Distribution of Scattered Projectiles for Grazing Collisions of Fast Atoms with a LiF(001) Surface

A. Schüller and H. Winter*

Institut für Physik, Humboldt Universität zu Berlin, Brook-Taylor-Strasse 6, D-12489 Berlin-Adlershof, Germany

(Received 26 June 2007; published 6 March 2008)

Fast atoms with keV energies are scattered under a grazing angle of incidence from a clean and flat LiF(001) surface. For scattering along low index azimuthal directions within the surface plane (''axial surface channeling'') we observe pronounced peak structures in the angular distributions for scattered projectiles that are attributed to ''supernumerary rainbows.'' This phenomenon can be understood in the framework of quantum scattering only and is observed here up to projectile energies of 20 keV. We demonstrate that the interaction potential and, in particular, its corrugation for fast atomic projectiles at surfaces can be derived with a high accuracy.

DOI: 10.1103/PhysRevLett.100.097602 PACS numbers: 79.20.Rf, 34.20.Cf, 68.49.Bc, 79.60.Bm

In collision physics the presence of *rainbows* is an interesting phenomenon that provides important details on the scattering process. In close analogy to the well-known atmospheric rainbow [1], enhancements for the flux of scattered particles are present whenever the angular deflection in the scattering shows an extremum. Then a substantial portion of incoming projectiles is scattered under a specific angle, the so-called *rainbow angle*. In different fields of physics rainbow effects have been studied. As an example, we mention here the scattering of atoms and ions with eV and keV energies from well-ordered crystal surfaces [2]. Recently, for the grazing impact of projectiles, detailed information on the interaction potentials for fast atoms in front of metal surfaces was derived from rainbow structures in an analysis based on classical trajectory calculations [3–6]. The main argument for neglecting quantum mechanical effects here, compared to thermal atom scattering [7], is the fact that in terms of matter waves the resulting de Broglie wavelength $\lambda_{dB} = h/M\upsilon$ (h = Planck constant, M = mass of particle, υ = velocity) [8] ascribed to keV atoms is below 0.01 Å (e.g., for ^{4}He atoms or ions of 10 keV kinetic energy: $\lambda_{dB} = 1.4 \times 10^{-3}$ Å), which is clearly smaller than the length scale for ordered structures at crystal surfaces of typically some Å. Furthermore, one expects for fast atoms substantial decoherence owing to excitations of projectile and target. Recent work, however, shows that the observation of diffraction with fast atomic projectiles is possible for grazing scattering from an insulator surface [9,10].

In this Letter we demonstrate that for grazing scattering of keV atoms from an insulator surface rainbow scattering is affected by quantum mechanical diffraction in terms of *supernumerary rainbows,* which have their origin in interference effects caused by the corrugation of the interaction potential at the surface. One finds such supernumerary rainbows as subtle additional structures observed for the atmospheric phenomenon [1,11], elastic atom-atom scattering at sub-eV energies [12,13], thermal atom scattering from surfaces [14–17], or elastic nuclear scattering at MeV energies [18]. For thermal He atom scattering (meV energies) from crystal surfaces [16], diffraction effects have been used to determine in detail the interaction potentials for atoms at surfaces [16,17,19,20]. From those studies the interaction potential for, e.g., He atoms in front of a LiF(001) surface has been deduced with a high level of sophistication for total energies in the meV domain.

Collisions of fast atoms or ions (keV energies and higher) with solids are generally discussed in terms of classical mechanics. Here fast atoms or ions are steered by strings (''axial channeling'') or planes of lattice atoms (''planar channeling'') in terms of small angle scattering [21,22]; one finds two vastly different regimes of scattering: a ''fast'' one for the motion parallel to atomic strings or planes with energy $E_{\|} = E_0\cos^2\Phi_{in} \approx E_0$ (E_0 is the projectile energy and Φ_{in} the glancing angle of incidence) and a ''slow'' normal motion with energy $E_{\perp} = E_0\sin^2\Phi_{in} \ll E_{\|}$ (for, e.g., $\Phi_{in} = 1$ deg is $E_{\perp} = 3 \times 10^{-4}E_0$). Both regimes of motion are widely decoupled, where for the transverse motion with low energy (velocity) the de Broglie wavelength is much larger than λ_{dB} attributed to the total velocity of the atomic particle. Furthermore, the suppression of excitations during grazing scattering from insulator targets with a band gap results in reduced energy loss and straggling compared to metals and to better defined final velocities and λ_{dB} as well as in less decoherence.

For observation of diffraction, a corrugation of the surface potential is needed as present for scattering along low index directions of atomic strings. This is illustrated in Fig. 1 by the sketch of equipotential contour lines in a plane normal to axial strings formed by F and Li atoms in the topmost surface layer (potential is averaged along strings). The periodicity of the surface potential follows the geometrical arrangement of surface atoms and is the origin of the diffraction pattern recently reported for axial surface channeling [9,10]. For channeling the velocity of

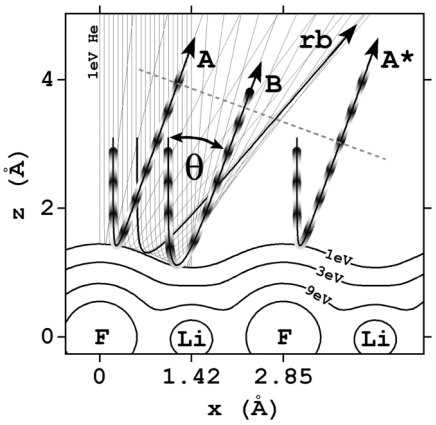

FIG. 1. Sketch of calculated trajectories in plane normal to atomic strings for scattering of ^{3}He atoms with $E_\perp = 1$ eV under the axial surface channeling from LiF(001) along ⟨110⟩. rb: trajectory for scattering under the rainbow angle; "A", "$A^\star$", "B" with the same deflection angle Θ. Patterns on trajectories indicate phase.

transverse motion is $v_\perp = v_0 \sin\Phi_{in}$ (v_0 = projectile velocity) so that diffraction can be considered with an enhanced de Broglie wavelength $\lambda_{dB\perp} = \lambda_{dB}/\sin\Phi_{in}$. For a periodicity length L of the potential, constructive interference holds for $n \cdot \lambda_{dB\perp} = L \cdot \sin\Theta$, with n being the diffraction order and Θ the deflection angle within the plane (cf. Fig. 1). In a semiclassical approach, this can be illustrated by interference between equivalent trajectories of type "A" and "$A^\star$" shown in Fig. 1. The resulting diffraction pattern has been reported recently in experiments on grazing scattering of atoms with total kinetic energies E_0 up to some keV from LiF(001) [9,10] and NaCl(001) surfaces [10].

In addition to interference of trajectories separated by the periodicity length L, scattering from a corrugated potential is affected by a second type of interference also sketched in Fig. 1. Below the rainbow angle of maximum deflection (trajectory "rb"), for each deflection angle Θ a pair of different trajectories can be found (e.g., trajectories "A" and "B" in Fig. 1). In a semiclassical approach [23], the phase difference between the two pathways determines the probability of scattering under a given angle Θ. This results in a characteristic intensity modulation of the diffraction pattern as established in studies with thermal He atoms [14–17]. In Fig. 1 the phase of matter waves is illustrated for trajectories "A" and "B" leading on the outgoing path to destructive interference and a reduction of intensity for scattering under this angle Θ. These oscillations are called supernumerary rainbows in analogy to the optical phenomenon in nature. We note that such supernumerary rainbow structures are related to a smaller coherence length so that they are still observed in a regime of fast atom scattering, where diffraction patterns based on the periodicity of the crystal lattice (trajectories "A" and "$A^\star$" in Fig. 1) cannot be resolved and excitations of surface and projectile might lead to considerable decoherence.

In our experiments we have scattered neutral He, N, Ne, and Ar atoms with energies up to 20 keV from a clean and well-ordered LiF(001) surface under a grazing angle of incidence Φ_{in} of typically 1°. The fast neutral beams were produced via neutralization of ions in a gas cell in front of a UHV chamber (base pressure some 10^{-11} mbar). The target surface was prepared by cycles of grazing sputtering with 25 keV Ar^+ ions at 250 °C and subsequent annealing to 350 °C. For axial surface channeling, the direction of the incident beam was aligned along a ⟨100⟩ (strings mixed of Li and F atoms) or ⟨110⟩ (strings of Li or F atoms) direction in the surface plane of the target. Two-dimensional angular distributions of scattered projectiles were recorded at a distance of 66 cm behind the target with a position sensitive channel plate detector [24].

In Fig. 2 we show 2D plots of angular distributions for scattering of 5.5 keV (lower panel), 7.3 keV (middle panel), and 8.6 keV (upper panel) ^{4}He atoms from LiF(001) along a ⟨100⟩ axial channel. The angle of incidence with respect to the surface plane is $\Phi_{in} = 0.71°$, which is decomposed for axial channeling in polar (azimuthal) incidence angles φ_{in} (ϑ_{in}) with $\Phi_{in}^2 = \varphi_{in}^2 + \vartheta_{in}^2$ (here $\vartheta_{in} = 0$). For elastic scattering holds $\Phi_{in}^2 = \Phi_{out}^2 = \varphi_{out}^2 + \vartheta_{out}^2$, with Φ_{out}, φ_{out}, ϑ_{out} being the corresponding exit angles. The data show structures in the angular distributions as a function of the deflection angle $\Theta = \arctan(\vartheta_{out}/\varphi_{out})$ located on a circle of radius Φ_{in} referred to the ⟨100⟩ strings. As for metal targets, one finds a

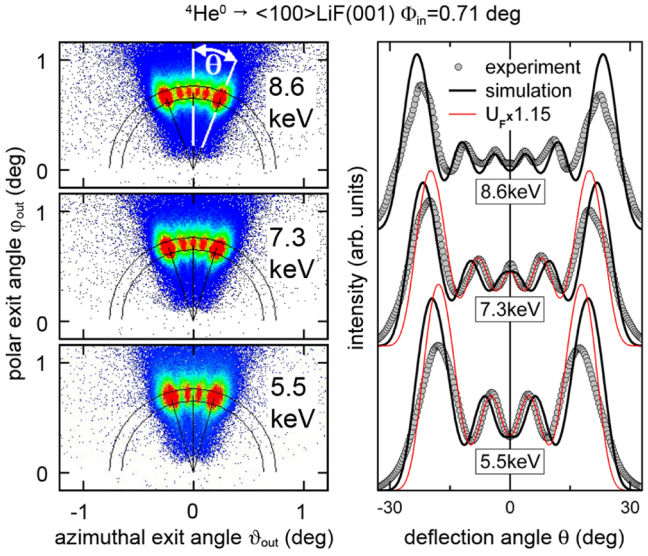

FIG. 2 (color online). Left panels: 2D intensity distributions for scattering of 5.5 keV (lower panel), 7.3 keV (middle panel), and 8.6 keV (upper panel) ^{4}He atoms from LiF(001) along ⟨100⟩ under $\Phi_{in} = 0.71°$. Color code: red = high intensity. Right panel: Projected intensities as a function of deflection angle Θ in the plane normal to the ⟨100⟩ axis. Curves: Results from semiclassical calculations.

pronounced peak at the corresponding classical "rainbow angle," which provides information on interatomic potentials between projectiles and atoms of the target surface [3–6]. Between the two outer peaks further peaks show up, which can be understood by quantum mechanical diffraction effects only in close analogy to the origin of supernumerary rainbows. These peaks were also observed for scattering of N, Ne, and Ar atoms where diffraction owing to the periodicity of the lattice could not be observed by us even at sub-keV energies.

A projection of the intensity on the deflection angle Θ within the annulus marked in the figure is shown in the right panel of Fig. 2. We reveal two (5.5 keV), three (7.3 keV), and four (8.6 keV) peaks in between the outer rainbow peaks. For the direction normal to the surface plane ($\Theta = 0$), we find a minimum for 5.5 keV and 8.6 keV, but a maximum at 7.3 keV. The curves represent results from semiclassical calculations outlined below.

The origin of atom diffraction for the observed structures can be demonstrated in a straightforward manner by making use of isotopes. For the same projectile energy and scattering geometry, ^{3}He and ^{4}He atoms probe the identical interaction potential and will have the same trajectories and angular distributions in terms of classical scattering. However, different masses and the resulting de Broglie wavelengths $\lambda_{dB} = h/Mv$ will lead to different phases and diffraction patterns for the supernumerary rainbow structures. As an example we show in Fig. 3 the projected intensity distributions for scattering of 3 keV ^{3}He and ^{4}He atoms from LiF(001) along ⟨110⟩ under $\Phi_{in} = 1.04°$, resulting in different oscillatory structures between the rainbow peaks that appear at the same angle. These features are reproduced by our semiclassical calculations (solid and dashed curves in Fig. 3).

In Fig. 4 we present as an example for heavier projectiles the 2D intensity distributions for 1 keV ^{20}Ne atoms scattered with $\Phi_{in} = 0.55°$ (lower panel) and 0.72° (upper panel) along ⟨110⟩ from a LiF(001) surface. Pronounced structures between the rainbow peaks can be resolved, as manifested in the right panel by projected intensities as a function of Θ, which are fairly well described by our simulations (solid curve).

We have analyzed our data in the framework of semiclassical theory developed for scattering of atoms from corrugated surfaces [23]. The overall interaction potential is constructed "pairwise additive" [20] by the summation of individual pair potentials for rare gas atoms and alkali or halide ions from theory [25], which agree on a quantitative level in the range of interest here (0.1 eV to 5 eV) with gas phase experiments and more accurate calculations [26–29]. Trajectories are obtained using concepts of classical mechanics where the effective potential results from an average along atomic strings [21]. A slight rumpling of 0.02 Å of the surface is taken into account [30]. The phases ψ of the associated plane matter waves are determined from the line integral of classical momentum along complete trajectories. The scattering amplitude for two different pathways leading to the same deflection angle Θ (cf. "A" and "B" in Fig. 1) is given by $\sqrt{\sigma_A}\exp(i\psi_A) + \sqrt{\sigma_B}\exp(i\psi_B)$ where the classical scattering cross sections σ are obtained from the simulations by the total number of trajectories within a given interval of Θ. The resulting diffraction patterns are convoluted with a Gaussian in order to take into account experimental and inherent broadening. This procedure does not shift peak positions of the supernumerary rainbows. The curves plotted in Figs. 2–4 represent results from these simulations.

The overall structures of observed diffraction patterns can be reproduced reasonably well by our calculations based on the Kim-Gordon potential [25] for atoms with ionic partners. We point out that the use of potentials between neutral atoms shows poor agreement with the

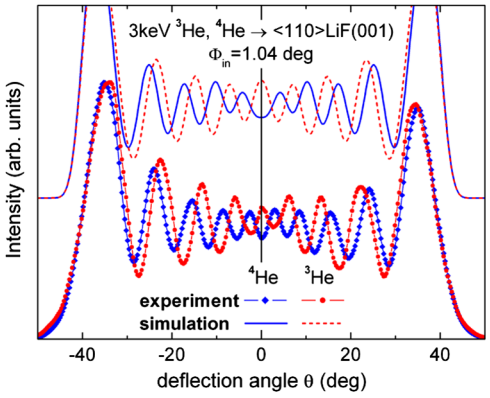

FIG. 3 (color online). Projected intensities as a function of deflection angle Θ in the plane normal to the ⟨110⟩ axis for scattering of 3 keV ^{3}He (circles) and ^{4}He atoms (diamonds) from LiF(001) under $\Phi_{in} = 1.04°$ along ⟨110⟩. Dashed (solid) curve: Semiclassical calculations for ^{3}He (^{4}He).

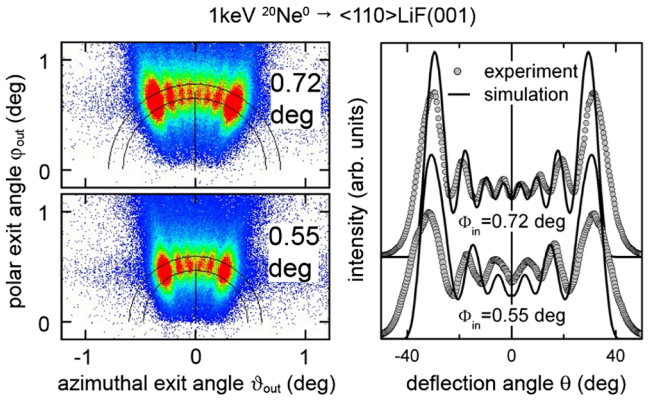

FIG. 4 (color online). Left panels: 2D intensity distributions for scattering of 1 keV ^{20}Ne from LiF(001) under $\Phi_{in} = 0.55°$ (lower panel) and 0.72° (upper panel) along ⟨110⟩. Right panel: Projected intensity as a function of the deflection angle Θ in the plane normal to ⟨110⟩. Solid curve: Results from semiclassical calculations.

data [31]. This is attributed to the ionic nature of the LiF crystal lattice and leads us to the aspect of the sensitivity of the observed diffraction pattern on the interaction potential and, in particular, on its corrugation. In passing we note that for the present systems the universal potential proposed by Ziegler, Biersack, and Littmark (ZBL potential) [32], often used for the description of collisions of fast atoms or ions in solids, is too repulsive for energies below 10 eV and the classical rainbow angle is smaller than 1° here. Also the extrapolation of potentials derived for the meV regime from thermal atom scattering [20] did not provide satisfactory results in our case.

A closer inspection of the data shown in Fig. 2 reveals a slight systematic shift between the peak positions observed in the experiment and the calculations using the Kim-Gordon potential [25]. The agreement with the experiment is clearly improved for this case, if, e.g., the He-F^- potential used is enhanced by 15%. This is equivalent to an outward shift of the equipotential plane for 0.83 eV ($E_0 = 5.5$ keV, $\Phi_{in} = 0.71°$) with a change of its corrugation amplitude from 0.066 Å to 0.084 Å by 0.018 Å. This clearly demonstrates the possibility of supernumerary rainbow structures to derive interatomic interaction potentials in the eV range for fast projectiles at surfaces with high sensitivity and accuracy by a kind of ''interferometric'' technique. Finally, we note that the Kim-Gordon potential and its modification was chosen here for a demonstration of the method only, a detailed analysis based on state of the art potentials has to be left to future work on this topic.

In conclusion, we have observed diffraction patterns for scattering of fast atoms with energies up to 20 keV from a LiF(001) surface under axial surface channeling. The interference effects are based on the corrugation of the atom surface potential, which can be derived with high accuracy from the diffraction patterns. These effects seem to be more robust against decoherence than diffraction for fast atoms due to the periodic structure of the crystal lattice.

We thank the DFG (Project No. Wi 1336) for financial support, and S. Wethekam, K. Maass, and J. Sölle for their assistance in the preparation of the experiments.

*Author to whom correspondence should be addressed.
winter@physik.hu-berlin.de

[1] J. D. Jackson, Phys. Rep. **320**, 27 (1999).
[2] A. W. Kleyn and T. C. M. Horn, Phys. Rep. **199**, 191 (1991).
[3] D. M. Danailov, R. Pfandzelter, T. Igel, and H. Winter, Nucl. Instrum. Methods Phys. Res., Sect. B **164/165**, 583 (2000).
[4] D. Danailov, K. Gärtner, and A. Caro, Nucl. Instrum. Methods Phys. Res., Sect. B **153**, 191 (1999).
[5] A. Schüller, G. Adamov, S. Wethekam, K. Maass, A. Mertens, and H. Winter, Phys. Rev. A **69**, 050901(R) (2004).
[6] A. Schüller and H. Winter, Nucl. Instrum. Methods Phys. Res., Sect. B **256**, 122 (2007).
[7] I. Estermann and A. Stern, Z. Phys. **61**, 95 (1930).
[8] L. V. de Broglie, Comptes Rendus **177**, 507 (1923).
[9] A. Schüller, S. Wethekam, and H. Winter, Phys. Rev. Lett. **98**, 016103 (2007).
[10] P. Rousseau, H. Khemliche, A. G. Borisov, and P. Roncin, Phys. Rev. Lett. **98**, 016104 (2007).
[11] R. L. Lee, Jr., Appl. Opt. **37**, 1506 (1998).
[12] U. Buck, H. O. Hoppe, F. Huisken, and H. Pauly, J. Chem. Phys. **60**, 4925 (1974).
[13] J. P. Toennies, Faraday Discuss. Chem. Soc. **55**, 129 (1973).
[14] M. J. Cardillo, Faraday Discuss. Chem. Soc. **80**, 17 (1985).
[15] M. J. Cardillo, G. E. Becker, S. J. Sibener, and D. R. Miller, Surf. Sci. **107**, 469 (1981).
[16] D. Farias and K. H. Rieder, Rep. Prog. Phys. **61**, 1575 (1998).
[17] G. Boato, P. Cantini, U. Garibaldi, A. C. Levi, L. Mattera, R. Spadacini, and G. E. Tommei, J. Phys. C **6**, L394 (1973).
[18] D. T. Khoa, W. von Oertzen, H. G. Bohlen, and S. Ohkubo, J. Phys. G **34**, R111 (2007).
[19] K. H. Rieder, N. Garcia, and V. Celli, Surf. Sci. **108**, 169 (1981).
[20] V. Celli, D. Eichenauer, A. Kaufhold, and J. P. Toennies, J. Chem. Phys. **83**, 2504 (1985).
[21] D. Gemmell, Rev. Mod. Phys. **46**, 129 (1974).
[22] H. Winter, Phys. Rep. **367**, 387 (2002).
[23] W. F. Avrin and R. P. Merrill, Surf. Sci. **311**, 269 (1994).
[24] Roentdek GmbH, Kelkheim-Ruppertshain, Germany.
[25] Y. S. Kim and R. G. Gordon, J. Chem. Phys. **60**, 4323 (1974).
[26] P. Polak-Dingels, M. S. Rajan, and E. A. Gislason, J. Chem. Phys. **77**, 3983 (1982).
[27] C. C. Kirkpatrick and L. A. Viehland, Chem. Phys. **98**, 221 (1985).
[28] M. T. Elford, I. Roeggen, and H. R. Skullerud, J. Phys. B **32**, 1873 (1999).
[29] B. R. Gray, T. G. Wright, E. L. Wood, and L. A. Viehland, Phys. Chem. Chem. Phys. **8**, 4752 (2006).
[30] J. Vogt and H. Weiss, Surf. Sci. **501**, 203 (2002).
[31] A. Schüller, K. Gärtner, and H. Winter, Europhys. Lett. **81**, 37007 (2008).
[32] J. F. Ziegler, J. P. Biersack, and U. Littmark, *The Stopping and Range of Ions in Solids* (Pergamon Press, New York, 1985), Vol. I.